

Transition between Quantum States in a Parallel-Coupled Double-Quantum-Dot

J.C. Chen¹, A.M. Chang^{1,*} and M.R. Melloch²

¹*Department of Physics, Purdue University,
West Lafayette, IN 47907*

²*School of Electrical and Computer Engineering,
Purdue University, West Lafayette, IN 47907*

(Dated: June 16, 2018)

Strong electron and spin correlations in a double-quantum-dot (DQD) can give rise to different quantum states. We observe a continuous transition from a Kondo state exhibiting a single-peak Kondo resonance to another exhibiting a double peak by increasing the inter-dot-coupling (t) in a parallel-coupled DQD. The transition into the double-peak state provides evidence for spin-entanglement between the excess-electron on each dot. Toward the transition, the peak splitting merges and becomes substantially smaller than t because of strong Coulomb effects. Our device tunability bodes well for future quantum computation applications.

PACS numbers: 73.23.-b, 73.63 Kv

The double-quantum-dot (DQD) is emerging as a versatile system for studying a variety of strongly correlated behaviors [1, 2, 3, 4, 5, 6, 7]. Following the experimental demonstration of the Kondo impurity-spin screening effect in single quantum dots [8, 9, 10, 11, 12, 13], recent theoretical investigations of the coupled-DQD system is uncovering new correlated behaviors [1, 2, 3, 4, 5, 6, 7]. These works suggest that the DQD enables a realization of the two-impurity Kondo problem first discussed in the context of metallic systems [1, 14, 15, 16] in which a competition between Kondo correlations and antiferromagnetic (AF) impurity-spin correlation leads to a quantum critical phenomenon. In a different regime of parameters, a related quantum critical phenomenon can occur driven by a competition between intra-dot Kondo coupling to leads and the inter-dot-coupling [2, 3]. In each scenario, a transition is predicted to occur between a quantum state characterized by a single-peaked Kondo resonance, and a different state with a double-peaked resonance. Depending on model and DQD geometry—whether series or parallel coupled—both a continuous or discontinuous [6] behavior in the Kondo peak characteristics have been predicted. The quantum transition in the two-impurity Kondo problem has received wide attention in the theoretical literature in the past two decades, to a large extent because the Kondo to antiferromagnetic transition involves an unusual *non-Fermi liquid* fixed point. Experimental investigation of this problem thus far has not been reported.

Here we describe transport properties of an artificial molecule formed by two-path, parallel-coupled double-quantum-dots, where the inter-dot-tunnel-coupling, t , can be tuned. In the Kondo regime the differential-conductance, dI/dV , exhibits a single peak centered at zero-bias for t comparable to the lead-coupling induced

level broadening. Increasing t by less than 10% resulted in a continuous evolution into a split Kondo resonance. At the same time the conductance at zero-bias exhibits a maximum in the vicinity of the transition. This peak splitting behavior in conjunction with distinct temperature dependences in the different regimes demonstrates a direct observation of an inter-dot-coupling-induced quantum transition. Moreover, on the double peak side *the zero-bias conductance becomes suppressed; this suppression represents direct evidence that the localized dot spins are becoming entangled into a spin singlet.*

While a double-peaked, coherent Kondo effect was observed by Jeong *et al.* in a series-coupled DQD geometry[17], the existence of a single-peaked Kondo effect at finite inter-dot-coupling has not previously been established. The series-geometry is unsuitable for an investigation of the transition because even a slight decrease in t can drastically reduce the tunnel current below detection. Therefore neither a single-peaked behavior nor a transition could be observed. Furthermore, direct evidence for spin-entanglement was not obtainable. In the parallel geometry the undesirable suppression of the conductance is avoided.

The Kondo effect in a single QD results from the coupling between the dot excess (unpaired) spin and the spin of the conduction electrons in the leads. The energy scale is given by the Kondo temperature $T_K \approx \sqrt{U\Gamma} \exp[-\pi|\mu - \epsilon_0|(U + \epsilon_0)/\Gamma U]$ where U is the on-site charging energy, ϵ_0 is the energy of the single-particle level, Γ reflects the dot level broadening from coupling to the leads, and μ is the chemical potential. The fully symmetric DQD system contains the additional inter-dot-coupling parameter, t . The two magnetic impurities, realized by a single excess-spin on each dot, interact through an effective AF coupling, $J = 4t^2/U$. The new energy scales, t and J , together with U , ϵ_0 , and Γ , introduce a rich variety of correlated physics. When U is the dominant energy scale as in the case of our quantum dots, for energies below U two different scenarios

*Electronic address: yingshe@physics.purdue.edu

are predicted for dots coupled in series [1, 2, 3, 4, 5, 6]. When $t < \Gamma$, the system can be cast [1] into the two-impurity Kondo problem initially discussed by Jones et al. [14, 15, 16]. The competition between Kondo effect and antiferromagnetism appears as a continuous phase transition (or crossover) at a critical value of the coupling $J/T_K \approx 2.5$. If however, t is tuned to $t > \Gamma$ before the AF transition point can be reached, the system undergoes a continuous transition from a separate Kondo state of individual spins on each dot (atomic-like) to a coherent bonding-antibonding superposition of the many-body Kondo states of the dots (molecular-like) [2, 3, 7]. Both the AF state and coherent bonding state exhibit a double-peaked Kondo resonance in the differential conductance versus source-drain bias and involve entanglement of the dot spins into a spin-singlet. Therefore they are likely closely related to one another. The parallel-coupled case has only recently been analyzed in a model without inter-dot-tunnel-coupling, t , where the AF coupling occurs via electrostatic coupling. A discontinuous jump in the differential conductance is predicted when the AF state becomes favored [6].

Our device was fabricated on $GaAs/Al_xGa_{1-x}As$ heterostructure containing a two-dimensional (2D) electron gas 80nm below the surface, with electron density and mobility of $n = 3.8 \times 10^{11} cm^{-2}$ and $\mu = 9 \times 10^5 cm^2/Vs$, respectively. The lithographic size of each dot is $170nm \times 200nm$ (see Fig. 1(a)). The eight separate metallic gates are configured and operated with five independently tunable gate voltages. The dark regions surrounding (and underneath) gates 5 represent 120nm thick over-exposed PMMA, which serve as spacer layers to decrease the local capacitance thus preventing depletion, enabling each lead to simultaneously connect to both dots. The experiment carried out at a lattice-temperature of 30mK. Standard, separate characterization of each dot in the closed dot regime [17] yielded a charging energy U of 2.517meV (2.95meV) for the left (right) dot, with corresponding dot-environment capacitance $C_\Sigma \approx 63.6af(54.3af)$, and level spacing $\Delta E \approx 219\mu eV(308\mu eV)$. Modeling the dot as a metal disk embedded in a dielectric resulted in disk of radius $r_e \approx 70nm(60nm)$ with 58 (43) electrons. To characterize the DQD and demonstrate the full tunability of our device, in Fig. 1(b) we show the Coulomb blockade (CB) charging diagram of the conductance versus plunger gates V2 and V4 [18] as t was increased, for weak coupling to the leads where Kondo correlation is unimportant. The central pincher gate V5 controlled t where a reduction of the gate voltage decreased t . At weak coupling (t small), the electrons separately tunnel through the two nearly independent dots forming grid like pattern, yielding rectangular domains in Fig. 1(b)(1). With increasing t charge quantization in individual dots is gradually lost as the domain vertices separated and the rectangles deformed into rounded hexagon. At large t when separate charge quantization is fully relaxed, the two dots merge into one and the domain boundaries become straight lines (Fig. 1(b)(6)). The evolution of the conductance pat-

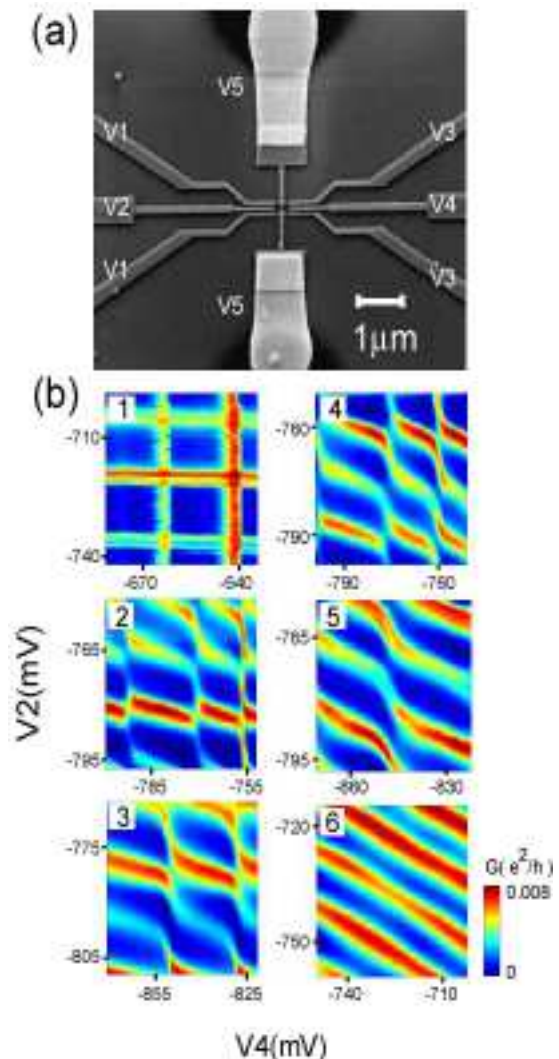


FIG. 1: Device and characterization in the CB regime: (a) Scanning electron micrograph of the device. (b) Logarithm of double dot conductance as a function of gate voltages V2 and V4 for weak lead-dot coupling. The color scale indicates the magnitude of conductance. The voltages in central pincher gate V5 are (1)-0.7477V (2)-0.6573V (3)-0.6534V (4)-0.6504V (5)-0.6494V (6)-0.5701V.

tern demonstrates the tunability of our DQD from ionic to covalent bonding states and bodes well for quantum computation applications [19].

The parameters Γ and t govern the delicate DQD Kondo physics. To obtain the necessary large t , the center pincher gate V5 was set so that the zigzag pattern in the charging diagram is barely visible (Fig. 2(a)), ensuring that the Kondo valleys can be located. To accomplish the formation of Kondo states in both dots, pincher gates V1 and V3 were tuned to give a sizable $\Gamma \approx \Delta E$ to ensure strong Kondo correlation. An estimate for t is based on the fact that the charging diagram indicates a configuration close to the limit of a merged, single large dot (Fig. 2(a)), so that the level broadening $\pi|t|^2/\Delta E$

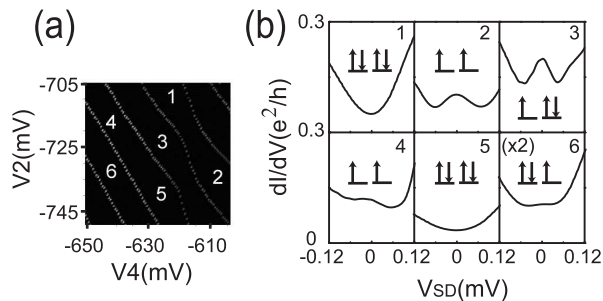


FIG. 2: Device characterization in the Kondo regime: (a) Charging diagram for the third cool-down depicted in a gray-scale plot of the conductance crest as a function of gate voltages V_2 and V_4 ($V_5 = -0.5965$ V). (b) Differential conductance traces from valleys 1 to 6 in Fig. 2(a). The insets indicate the spin configuration of the uppermost, occupied electronic levels on each dot. Note that a single upward-pointing arrow only denotes an unpaired electron, and is not intended to represent the actual direction of spin alignment.

should be comparable to the level spacing ΔE , yielding $t \approx 150 \mu eV$, while Γ is deduced to be $\approx 150 \mu eV$ from the half-width of the Coulomb blockade peaks.

Care is required when changing t . The mutual capacitive coupling between the gates and dots gives rise to a complex capacitance matrix. Operating V_5 to tune t simultaneously affected the charge on the dots and other gates. Furthermore, slight residual asymmetry in the coupling to the leads caused the maximum of the Kondo zero-bias anomaly (ZBA) in the dI/dV to occasionally occur at nonzero voltages $V_{SD} \neq 0$ (termed the anomalous Kondo effect [20]). By adjusting a combination of the remaining gates we tuned the ZBA to be nearly symmetrical about zero-bias. For practical purposes we relied on plunger-gates V_2 or V_4 , which were found to follow V_5 in an approximately linear manner. This procedure can be thought as experimentally diagonalizing the capacitance matrix. The desired configuration of an unpaired excess-spin on each dot could be maintained within a tuning range of $\approx 4 \sim 7$ mV in V_5 without causing a sudden change in the charge configuration. Note that V_5 is set typically ≈ 70 mV above pinch-off. Therefore the relative tuning range in this Kondo regime is roughly 6-10% of closure and even smaller for the corresponding fractional change in t , since tunnel-coupling becomes exponentially suppressed in the small value limit.

Three distinct spin configurations may appear assuming even-odd electron filling and focusing on the top-most states in each dot (Fig. 2(b)). Our investigation was carried out in such regimes. Non even-odd behavior was also observable, but will not be discussed [21]. The Kondo valleys and spin states in each dot were identified by measuring the differential conductance, dI/dV , versus source-drain bias, V_{SD} , at an electronic temperature of ~ 40 mK. For regions 1-6 in Fig. 2(a), we observed the expected appearance and disappearance of Kondo resonance peaks near zero-bias shown in Fig. 2(b).

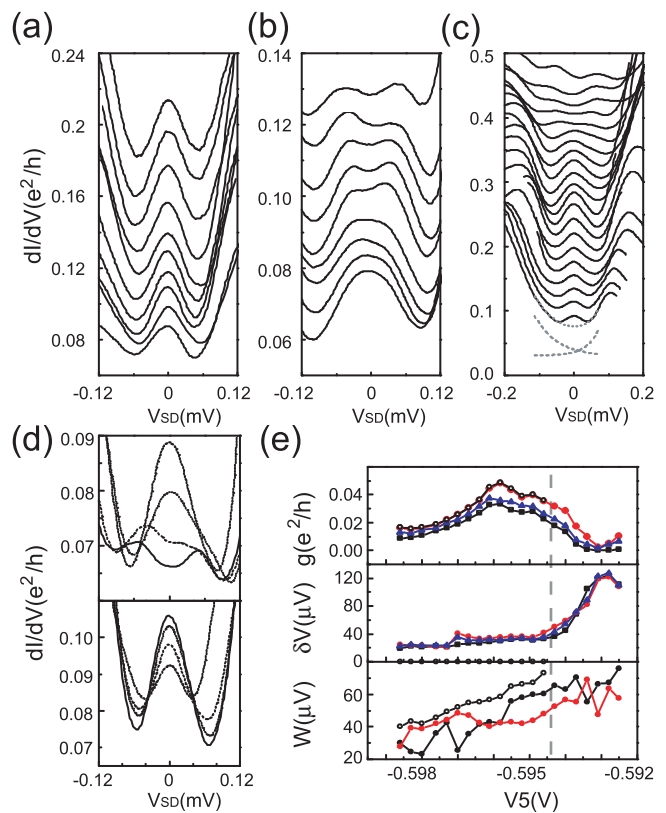


FIG. 3: The differential conductance, dI/dV , versus V_{SD} for different inter-dot coupling strength tuned via V_5 gate. (a) From top to bottom: $V_5 = -0.6155, -0.616, -0.6165, -0.617, -0.6175, -0.618, -0.6185, -0.619, -0.6195, -0.62$ V, second cool-down. (b) From top to bottom: $V_5 = -0.5965, -0.5970, -0.5975, -0.5978, -0.5982, -0.5987, -0.5990, -0.5992, -0.5995$ V, first cool-down, offset by $0.005e^2/h$ for each trace. (c) From top to bottom: $V_5 = -0.5925, -0.5928, -0.5931, -0.5934, -0.5937, -0.5940, -0.5943, -0.5946, -0.5949, -0.5952, -0.5955, -0.5958, -0.5961, -0.5964, -0.5967, -0.5970, -0.5973, -0.5976, -0.5980, -0.5983, -0.5986$ V, third cool-down as measured in Kondo valley 2 of Fig. 2(b), offset by $0.02e^2/h$ for each trace. The traces vary in different cool-downs due to the rearrangement in the occupation of charged in defects and traps. (d) Selected data from (c) without offset. Bottom half shows first quantum state regime (from top to bottom: $V_5 = -0.5961, -0.5964, -0.5970, -0.5986$). The upper half shows the second regime (from top to bottom: $V_5 = -0.5946, -0.5940, -0.5937, -0.5934$). (e) ZBA peak amplitude $g = dI/dV|_{V=0}$, peak splitting δV and width W extracted by first subtracting three types of background signals followed by a two-Gaussian fit. The fit and data are virtually indistinguishable. The simulated backgrounds are \bullet : two exponential functions + constant (e.g. marked by the two gray dash lines for the bottom trace in (c) and combined functions shown as gray dot line); \blacktriangle two Boltzmann and \blacksquare linear function. The bottom figure shows the two peak widths obtained after the subtraction of a two exponential background. Results for a single Gaussian fit ($V_5 < -0.594$ V only) are indicated by open-circles (\circ). Typically, the fitting error is smaller than the symbol.

When t was tuned two distinct regimes of behavior were evident in dI/dV (see Fig. 3(a)-(d)). The main features in the first regime (see Fig. 3(a),(d) bottom half) were the clear presence of a single peak in the ZBA, an increasing peak width and an increasing linear conductance $g = dI/dV|_{V=0}$ with increasing t . In the second regime where t was increased further (see Fig. 3(b), (d) upper half), the single ZBA peak developed into two peaks. In some Kondo valleys, both types of behavior were observed as shown in Fig. 3(c),(d), in which the transition is seen to take place in a continuous manner. In the transition region, the ZBA peak broadened and its zero-bias value, g , approached a maximum, became flat before dropping as the ZBA peak gradually split into two. The suppression of g on the double-peaked side can be attributed to the emergence of spin-singlet correlation between the two dot spins [1, 2, 3, 4, 5, 6, 7]. The maximum g is about $\sim 0.1e^2/h$, reduced below the theoretical unitary limit of $4e^2/h$. This reduction can occur when the energy levels in the two dots differ and the dot-lead coupling is asymmetric [3, 22].

Analyzing the transition with detailed curve fitting we quantify the amplitude, splitting and width of the ZBA peak(s) at each V_5 gate voltage within well-defined bounds. In the absence of precise theoretical functional forms either for the conductance background or the ZBA peak itself, we first systematically subtracted three sensible backgrounds. After subtraction of each background we fitted the ZBA using three (combined) peak shapes: one (or two) Gaussian, Lorentzian and the Breit-Wigner resonance form. The resultant parameters invariably exhibited similar trends as shown in Fig. 3(e). The double-peak feature visibly disappeared at $V_5 \sim -0.594V$ as indicated by the dash line, and roughly coincides with the g maximum position. Note that the peak splitting, δ , dramatically reduces from a maximum of $\sim 120\mu eV$ to ~ 0 when V_5 is slightly reduced from $-0.5925V$ to $\sim -0.595V$ and correspondingly t is reduced by less than 4% from an initial value $t \approx 150\mu eV$.

In addition to differences in the peak shape the temperature dependence of dI/dV was also distinct in the two regimes (see Fig. 4). In the single peak regime, the zero-bias dI/dV , $g(T)$, decreased logarithmically with T (Fig. 4(a)). In contrast, when double peaks appeared, $g(T)$ exhibited a non-monotonic behavior (Fig. 4(b)), where with increasing T $g(T)$ slightly increased initially, then slowly decreased before increasing again when T exceeded T_K . Together, these evidences point to qualitatively different phases in the two regimes and the existence of a quantum transition between them.

To date no theoretical work has addressed the parallel-coupled DQD with inter-dot tunnel coupling. Nevertheless, because the ZBA occurs under slightly non-equilibrium conditions it is likely that we may identify the observed transition with the quantum critical phenomenon discussed in the two-impurity Kondo problem

for the series geometry based on the following evidence: (a) a continuous evolution from the single- to double

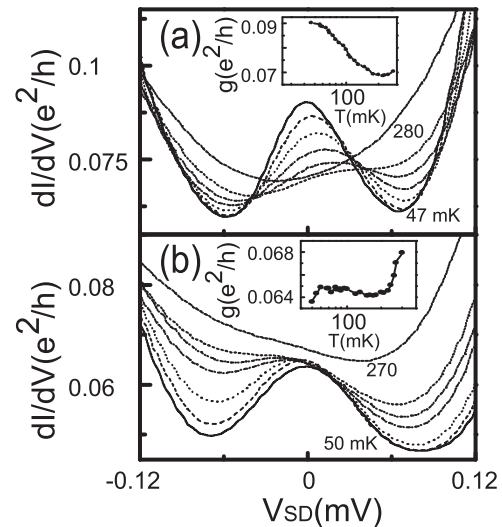


FIG. 4: Temperature dependence of the differential conductance dI/dV versus V_{SD} in the Kondo valley of Fig. 3(c): (a) First quantum state regime: from top to bottom $T=47, 70, 95, 110, 150, 180, 220, 280$ mK, at $V_5=-0.5953V$. (b) Second quantum state regime: from bottom to top $T= 50, 80, 100, 160, 180, 210, 250, 270$ mK, at $V_5=-0.5928V$. Insets show the distinctly different temperature dependences of the zero-bias linear conductance, $g(T) = dI/dV|_{V=0}$, in the two regimes.

peaked behavior, (b) a maximum in g , the zero-bias dI/dV , near the transition point, (c) different behaviors in the temperature dependence of g , and (d) a strong renormalization of the peak splitting, δ , compared to the estimated t or AF coupling, J , close to the transition. These features are all in qualitative agreement with predictions for a series-coupled DQD [1, 2, 3, 4, 5, 6, 7, 22], although ideally theory predicts a maximum g reaching the unitarity limit $4e^2/h$. Semi-quantitatively, it is informative to roughly estimate key parameters and compared these to observed splitting, $\delta \leq 120\mu eV$. Within the theoretical scenarios, δ must be compared to $4t \approx 600\mu eV$ or $2J = 8t^2/U \approx 180\mu eV$. (Note that in the open dot regime U is expected to be reduced from its closed dot value by roughly 1/3 [11], yielding $U \approx 1meV$.) The reduction of δ compared to $4t$ and $2J$ are in agreement with theory and lends further credibility to our identification of the quantum transition.

Acknowledgements We thank H. Baranger, K. Matveev, S. Khlebnikov, N. Giordano, N. Windgreen, D. Cox, A. Schiller, and H. Nakanishi for discussions, and F. Altomare, L.C. Tung, V. Gusiatnikov, and H. Jeong for assistance in the experiment. Work supported by NSF grants DMR-9801760 and DMR-0135931.

-
- [1] A. Georges, and Y. Meir, Phys. Rev. Lett. **82**, 3508 (1999).
- [2] R. Aguado, and D.C. Langreth, Phys. Rev. Lett. **85**, 1946 (2000).
- [3] T. Aono, and M. Eto, Phys. Rev. B **63**, 125327 (2001).
- [4] B. Ding, and L.L. Lei, Phys. Rev. B **65**, 241304 (2002).
- [5] W. Izumida, and O. Sakai, Phys. Rev. B **62**, 10260 (2000).
- [6] R. López *et al.*, Phys. Rev. Lett. **89**, art no. 136802 (2002).
- [7] C.A. Bússer *et al.*, Phys. Rev. B **62**, 9907 (2000).
- [8] D. Goldhaber-Gordon *et al.*, Nature **391**, 156 (1998).
- [9] S.M. Cronenwett *et al.*, Science **281**, 540 (1998).
- [10] S. Sasaki *et al.*, Science **405**, 764 (2000).
- [11] W.G. van der Wiel *et al.*, Science **289**, 2105 (2000).
- [12] Y. Ji *et al.*, Science **290**, 779 (2000).
- [13] J. Nygard *et al.*, Nature **408**, 342 (2000).
- [14] B.A. Jones, and C.M. Varma, Phys. Rev. Lett. **58**, 843 (1987).
- [15] B.A. Jones *et al.*, Phys. Rev. Lett. **61**, 125 (1988).
- [16] I. Affleck, and A.W.W. Ludwig, Phys. Rev. Lett. **68**, 1046 (1992).
- [17] H. Jeong, A.M. Chang, and M.R. Melloch, Science **293**, 2221 (2001).
- [18] C. Livermore *et al.*, Science **274**, 1332 (1996).
- [19] D. Loss, and D.P. DiVincenzo, Phys. Rev. A **57**, 120 (1998).
- [20] F. Simmel *et al.*, Phys. Rev. Lett. **83**, 804 (1999).
- [21] J. Schmid *et al.*, Phys. Rev. Lett. **84**, 5824 (2000).
- [22] R. Aguado, and D.C. Langreth, cond-mat/0207283.